MIJST
MIST International Journal of Science and Technology

The Influence of Silt Layer Orientation on Slope Stability in Shale Formations

AKM Badrul Alam[1*], Yoshiaki Fujii[2], Zhixue Li[3], Nahid Hasan Dipu[4], Md. Tajib–Ul–Islam[5], Shakil Ahmed Razo[6]

[1,4-6]Department of Petroleum and Mining Engineering, Military Institute of Science and Technology, Dhaka, Bangladesh
[2]Faculty of Engineering, Hokkaido University, Japan
[3]School of Energy Science and Engineering, Henan Polytechnic University, China

Corresponding Email: *badrul.alam@pme.mist.ac.bd*

ARTICLE INFO

Article History:

Received: 05th May 2025
Revised: 02nd June 2025
Accepted: 03rd June 2025
Published: 30th June 2025

Keywords:

Shale rock masses
Silt layers
Slope stability
Elasto-plastic model
Temporal degradation

ABSTRACT

Shale rock masses often include silt layers, impacting slope stability in construction and mining. Analyzing their interaction is crucial for long-term stability. This study used an elasto-plastic model, incorporating the stress transfer method and Coulomb's criterion. It computed stress distribution, assessed failure potential, and identified vulnerable regions. A shale rock mass ranging from 14.75 to 16.75 meter thick, with silt layers varying from 0.36 to 0.5 meter thick was considered in the model. It examined four silt layer conditions: horizontal (SilHL), vertical (SilVL), in-facing (SilIN), and out-facing slope (SilOUT). Mechanical parameters like Uniaxial Compressive Strength (UCS), Tensile Strength (TS), and Young's modulus (E) were adjusted for varied scenarios: UCS (0.5 to 5 MPa), and E (6 to 60 MPa), keeping UCS/TS = 5 for all the conditions. In the elasto-plastic analysis, overall reductions of 20%, 40%, 60%, 80%, and 90% in E, UCS and TS were evaluated, taking into consideration the temporal degradation. The findings for SilHL indicate that: (i) when the E, UCS, and TS of the silt layer and shale were equivalent, significant structural failure occurred at 60% reduction, with pronounced collapse at 80% and complete failure at 90%; (ii) a lower E in the silt layer with equivalent strength to shale showed no significant differences; (iii) reductions in both E and UCS for the silt layer also revealed no notable differences. For SilVL, the results were similar, with (i) consistent effects as SilHL; (ii) slippage occurring with a lower E for the silt layer; and (iii) bitension failure and toppling observed when the silt layer's strength was one-tenth that of shale. In SilIN, similar patterns emerged, with slippage and tension failures noted under reduced E and UCS conditions. For SilOUT, results mirrored SilHL, with tension failures and divergence in failure patterns under reduced E and UCS. The results of this study indicate that slope failure scenarios involving shale with a silt layer can be effectively simulated using the elasto-plastic method, particularly by incorporating reductions in strength and Young's modulus. Furthermore, these findings highlight the critical need for additional research on specific slope configurations to refine design methodologies and enhance stability assessments within the context of the elasto-plastic model.

1. INTRODUCTION

Shale is characterized by its fine-grained, layered structures, often interspersed with silt layers that significantly influence slope stability in construction and mining projects. The presence of these silt layers introduces discontinuities and potential planes of weakness within the rock mass, thereby compromising its overall strength and increasing the likelihood of slope failures. The interaction between the shale matrix and the silt layers is complex, influenced by various factors, including the orientation, thickness, and mechanical properties of the silt layers, as well as in-situ stress conditions and environmental factors. Understanding the mechanical behavior of silt layers within shale rock masses is crucial for ensuring long-term stability.

The impact of these silt layers on slope stability has been the subject of academic inquiry, yielding critical insights into their mechanical behavior. Research highlights the significance of elastic modulus and shear strength in maintaining slope stability, revealing that even minor reductions in these parameters can lead to substantial changes in slope behavior (Duncan et al., 2014). The complex interplay between shear and tensile failures in inclined slopes, particularly those influenced by silt layers, further illustrates the multifaceted nature of slope failure mechanisms (Bishop, 1955).

The stability of shale formations is a critical concern in engineering fields. Although extensive research has been conducted on the influence of various factors affecting this issue in petroleum engineering, there is a notable lack of studies specifically addressing slope stability. Brittleness, which significantly affects stability, is influenced by mineral content, organic matter, bedding, and porosity (Li, 2022). Stress unloading during drilling can weaken shale strength, with increased confining pressure and axial stress exacerbating this effect (Ding et al., 2023). Additionally, elevated temperatures (over 200°C) and higher tectosilicate or carbonate content can enhance fault instability (Zhang et al., 2022). Bedding planes, hydration, and stress unloading collectively impact wellbore stability (Ding et al., 2023). The complex pore structure of shale leads to dual-pore pressure and dual-effective stress behavior, complicating stability analyses (Mehrabian et al., 2019). Understanding these factors is essential for optimizing drilling operations and assessing exploration risks (Li, 2022; Mehrabian et al., 2019). This study focuses on the stability of shale slopes concerning the orientation of the underlying silt layer from rock engineering point of view.

Key internal factors affecting slope stability include unit weight, cohesion, and internal friction angle (Harabinova & Panulinova, 2022; Hulagabali, 2019; Wen et al., 2012). Slope geometry, particularly height and angle, significantly influences stability (Deris et al., 2020). Water presence can destabilize shale, leading to rapid degradation (Alam et al., 2021). Geological structures and human activities also contribute to instability (Akoudad et al., 2024). The factors contributing to the reduction in strength and Young's modulus in relation to shale slope stability have not yet been adequately explored.

A critical consideration is the long-term impact of weathering and environmental factors on shale slopes. Laboratory studies have demonstrated that water saturation significantly affects the Young's modulus and unconfined compressive strength (UCS) of shale (Alam et al., 2021; Li et al., 2016). This study investigates the reduction in strength and Young's modulus (Table 1) concerning the stability of shale slopes to integrate these potential influences into slope stability analyses to ensure the long-term safety and performance of engineered structures within shale formations.

Table 1: Young's modulus (E) and Strength (S) (MPa) of the shale and silt layer. The ratio is UCS/TS; uniaxial compressive strength (UCS) and tensile strength (TS)

			Decrement in engineering properties					
Analysis	**Conditions**	**Rock/ layer**	**0%**	**20%**	**40%**	**60%**	**80%**	**90%**
Elastic	Same E	Shale	60	-	-	-	-	-
		Silt	60	-	-	-	-	-
	Lower E	Shale	60	60	60	60	60	60
		Silt	60	48	36	24	12	6
Elasto-plastic	Same E and Same S	Shale	60, 5/1	60, 4/.8	60, 3/.6	60, 2/.4	60, 1/.2	60, .5/.1
		Silt	60, 5/1	60, 4/.8	60, 3/.6	60, 2/.4	60, 1/.2	60, .5/.1
	Lower E and Same S	Shale	60, 5/1	60, 4/.8	60, 3/.6	60, 2/.4	60, 1/.2	60, .5/.1
		Silt	60, 5/1	48, 4/.8	36, 3/.6	24, 2/.4	12, 1/.2	6, .5/.1
	Lower E and Lower S	Shale	60, 5/1	60, 4/.8	60, 3/.6	60, 2/.4	60, 1/.2	60, .5/.1
		Silt	60, .5/.1	48, .4/.08	36, .3/.06	24, .2/.04	12, .1/.02	6, .05/.01

Numerical modeling approaches have proven invaluable, providing simulations that demonstrate how silt layers significantly alter stress distribution and failure mechanisms within slopes (Zhang et al., 2018). Complementary field investigations reveal the real-world implications of silt-rich shale formations, which are prone to triggering landslides (Lee et al., 2015). Consequently, rigorous geotechnical assessments in regions characterized by silt layers are imperative to enhance prediction accuracy and design safety. This underscores the necessity of integrating the characteristics of silt layers into slope stability models (Fell et al., 2005). The present study focuses on the temporal degradation of strength and Young’s modulus in these layers through elasto-plastic analysis, aiming to further elucidate the implications of silt interlayers on slope stability in shale formations.

2. MATERIALS AND METHOD

The present study investigated the mechanical behavior of a shale rock mass containing silt layers, employing an elasto-plastic model that incorporated stress transfer method and the Coulomb’s failure criterion for interpreting the complex behavior associated with silt layer-induced instability in shale rock masses.

The elasto-plastic analysis uses the stress transfer method (Akai & Hori, 1978). Initially, the stress components of the material are calculated using elastic principles. Following this, the stress state of each element is compared against Coulomb's criterion to determine potential failure (Fig. 1). If the criterion indicates failure, the axial stress drop is then calculated based on this failure criterion. Then the nodal forces resulting from the axial stress drop are computed by the equation (1) and applied to nodes.

$$F = \int B^T \Delta\sigma \, dV \quad (1)$$

$$\varepsilon = BU \quad (2)$$

where, F represents the nodal force vector, Δσ is the vector for the stress drop, V is the volume of the element, B^T is the transposed matrix of B, B is the strain-displacement matrix, ε is the strain vector and U is the nodal displacement vector. This procedure is iterated until the solution converges.

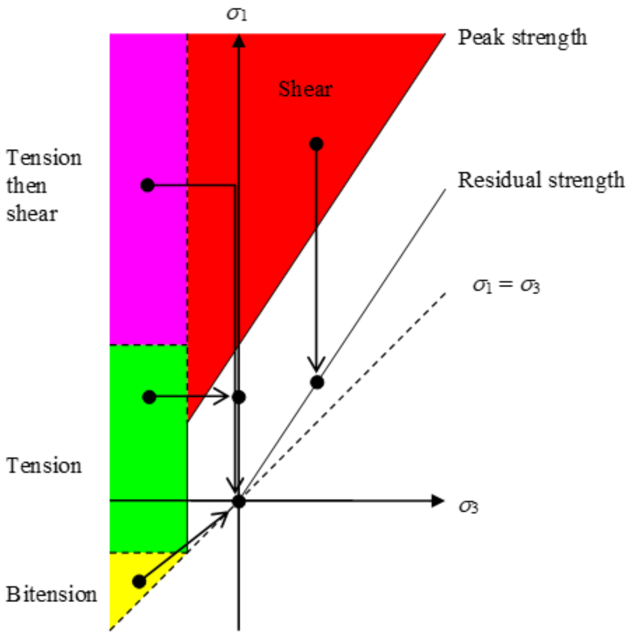

Figure 1: Failure criterion of the elasto-plastic analysis

The shale rock mass under consideration varied in thickness from 13.50 to 16.75 meters, and the embedded silt layers ranged from 0.36 to 0.5 meters in thickness. The boundary conditions for the analysis are illustrated in Fig. 2 for SilHL and are consistent across all cases.

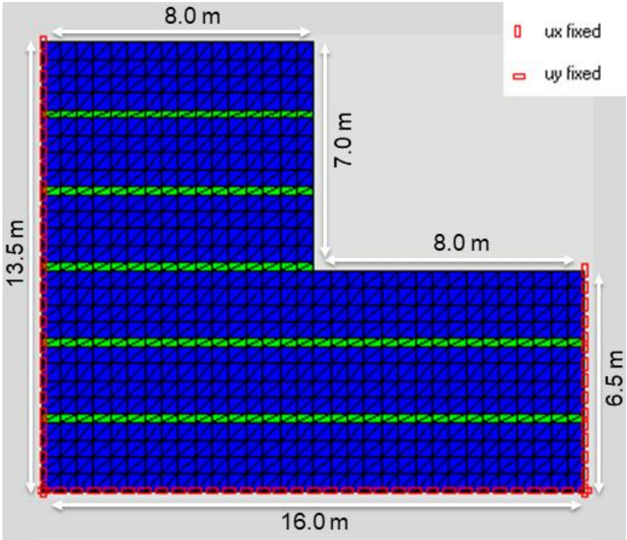

Figure 2: The boundary condition for the numerical analysis of SilHL is consistent across all cases

The study focused on four distinct silt layer configurations: horizontal (SilHL), vertical (SilVL), inclined against the slope (SilIN), and inclined along the slope (SilOUT). The mechanical properties of the silt layers, including uniaxial compressive strength (UCS), tensile strength (TS), and Young's modulus (E), were systematically varied to simulate a range of scenarios, with UCS values between 0.5 and 5 MPa, TS values were kept at UCS/TS = 5 and E values between 6 and 60 MPa. The mechanical properties under the conditions are summarized in Table 1. This comprehensive approach allowed for a thorough evaluation of the complex interactions between silt layer orientation, mechanical properties, and the overall stability of the shale rock mass by the elasto-plastic model.

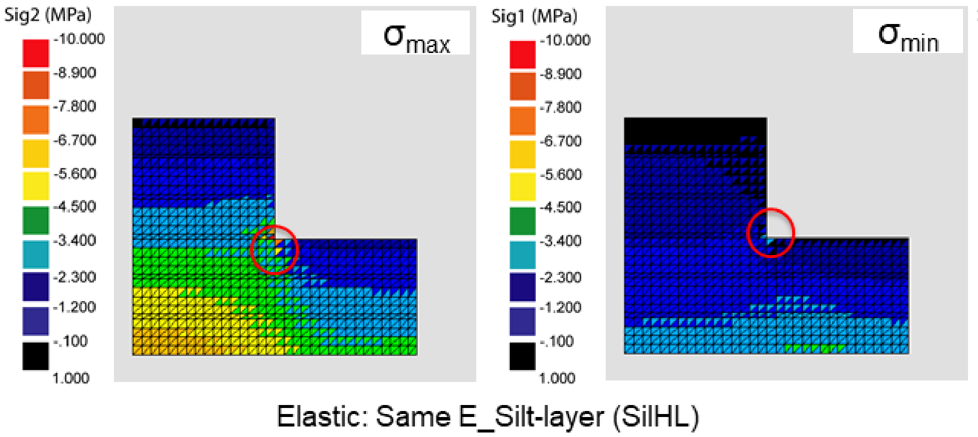

Figure 3: Elastic analysis of the slope cases for same E. The circle representing the stress concentrated area at the base

3. RESULTS AND DISCUSSION

3.1 Elastic Analysis

When shale and silt layers exhibit identical elastic moduli (E), stress concentrations are observed predominantly at the bases of these layers (Fig. 3). In scenarios where the silt layer possesses a lower elastic modulus than the shale, only marginal changes in the maximum stress (σ_{max}) are noted for the SilHL, SilIN and SilOUT configurations (Fig. 4 serves as an example for SilHL). Conversely, a pronounced decrease in σ_{max} is evident within the silt layer at the SilVL configuration (Fig. 5).

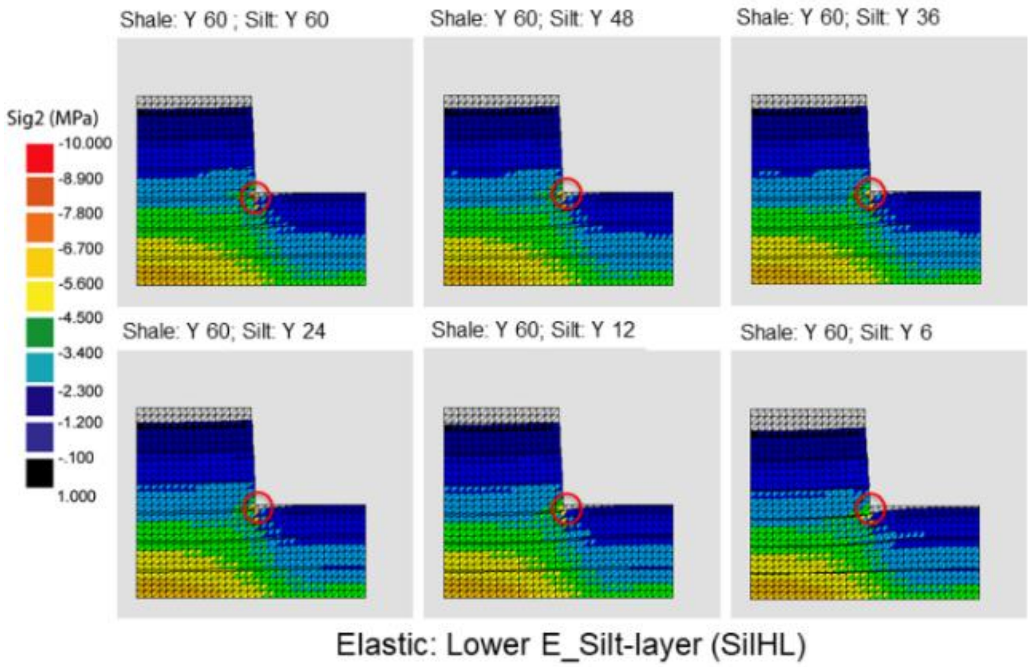

Figure 4: Elastically analyzed σ_{max} of the slope cases for lower *E* for silt layers. The circle representing the stress concentrated area at the base

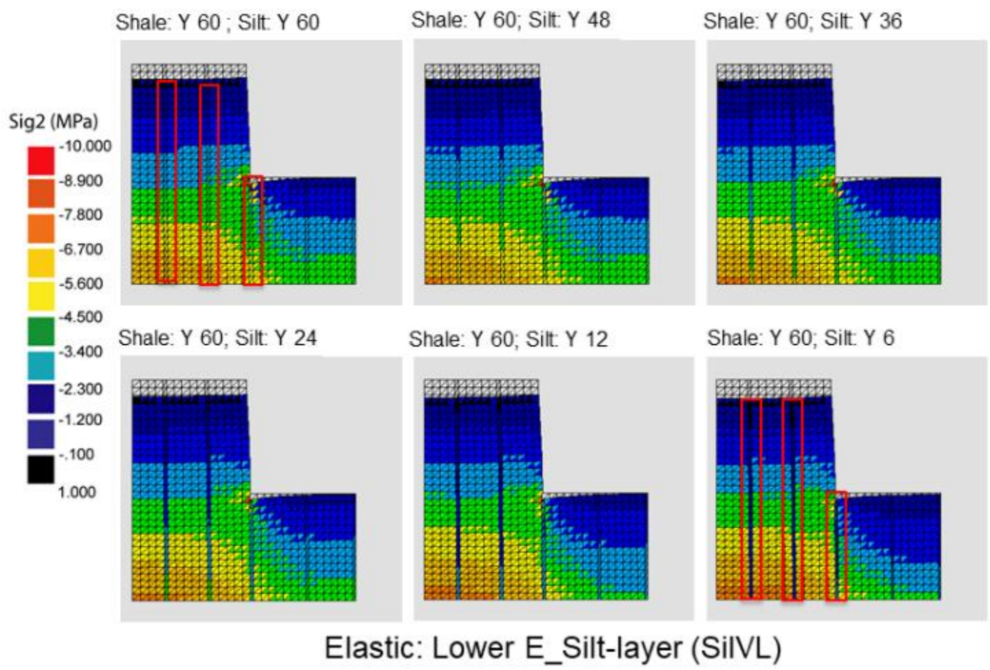

Figure 5: Elastically analyzed σ_{max} of the slope cases for lower E for silt layers. The rectangle representing the stress concentrated area at the base

3.2 Elasto-plastic Analysis

In the case of horizontal silt layer (SilHL), when both the elastic modulus (*E*) and strength are the same, shear failure is observed from 40% decrease in mechanical properties occurs (Fig. 6a).

As the mechanical properties decrease further, element failure escalates significantly with deformation. When the silt elastic modulus is lowered while the strength is the same (Fig. 6b), the initial condition remains unchanged with no deformation; however, slight increases in deformation are noted as mechanical properties decrease. In scenarios where both the elastic modulus and strength of silt are lower, shear failure of the silt layer is observed from the beginning (Fig. 6c). However, the failure does not extend and similar deformation is observed.

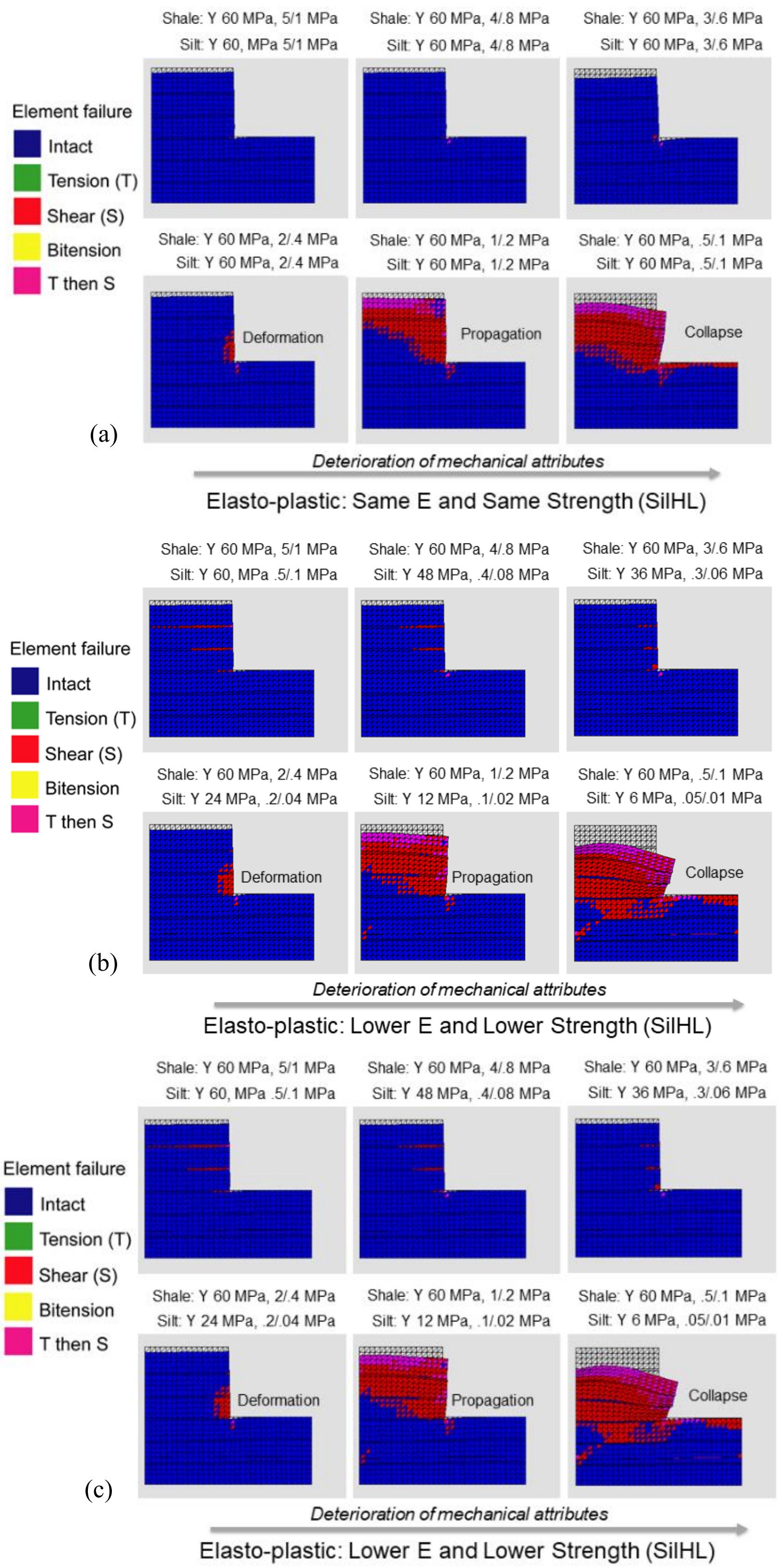

Figure 6: Elasto-plastically analyzed element failure and deformation in different conditions for horizontal silt layer (SilHL). Y: Young's modulus, UCS/TS

For the vertical silt layer (SilVL), the behavior mirrors that of SilHL under similar conditions. The initial shear failure near the base indicates vulnerability, with subsequent increases in shear failures as mechanical properties decline (Fig. 7a). When the elastic modulus of the silt is lowered while the strength is the same, deformation patterns are similar to the previous case, yet significant slip leading to toppling is noted at higher decrements (Fig. 7b). In cases where both mechanical properties of the silt are reduced, shear failures are prominent, accompanied by larger slip and complex failure modes (Fig. 7c).

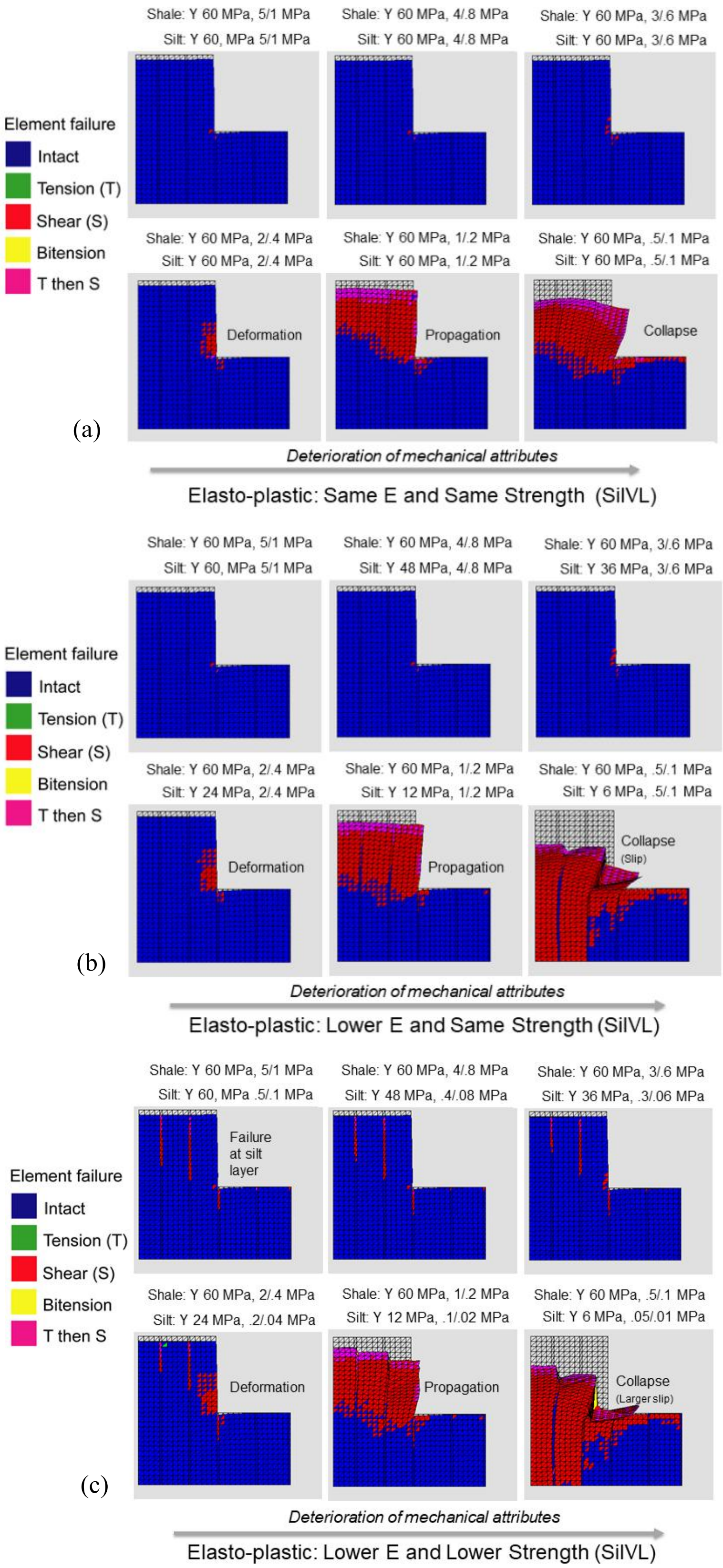

Figure 7: Elasto-plastically analyzed element failure and deformation for vertical silt layer (SilVL)

The in-facing silt layer case (SilIN) displays its own unique characteristics. Here, the initiation of shear failure at the base suggests instability, with increasing deformation and transitions to tension then shear failures as mechanical properties decrease (Fig. 8a).

Similar responses are observed when the silt elastic modulus is lowered while the strength is the same, though increased deformation is noted at higher mechanical property decreases and toppling-like failure was observed (Fig. 8b). In conditions where both properties of the silt are reduced, the trend of failure escalates significantly (Fig. 8c).

For the out-facing slope (SilOUT), initial shear failures escalate to total collapse scenarios as mechanical properties decrease, indicating extreme vulnerability. When the silt strength is lowered while the silt elastic modulus remains unchanged (Fig. 9a), results diverge significantly, highlighting instability under lower elastic constant (Fig. 9b). In cases where both properties of the silt are reduced, larger deformation leads to non-converging solutions, emphasizing the critical nature of these conditions (Fig. 9c).

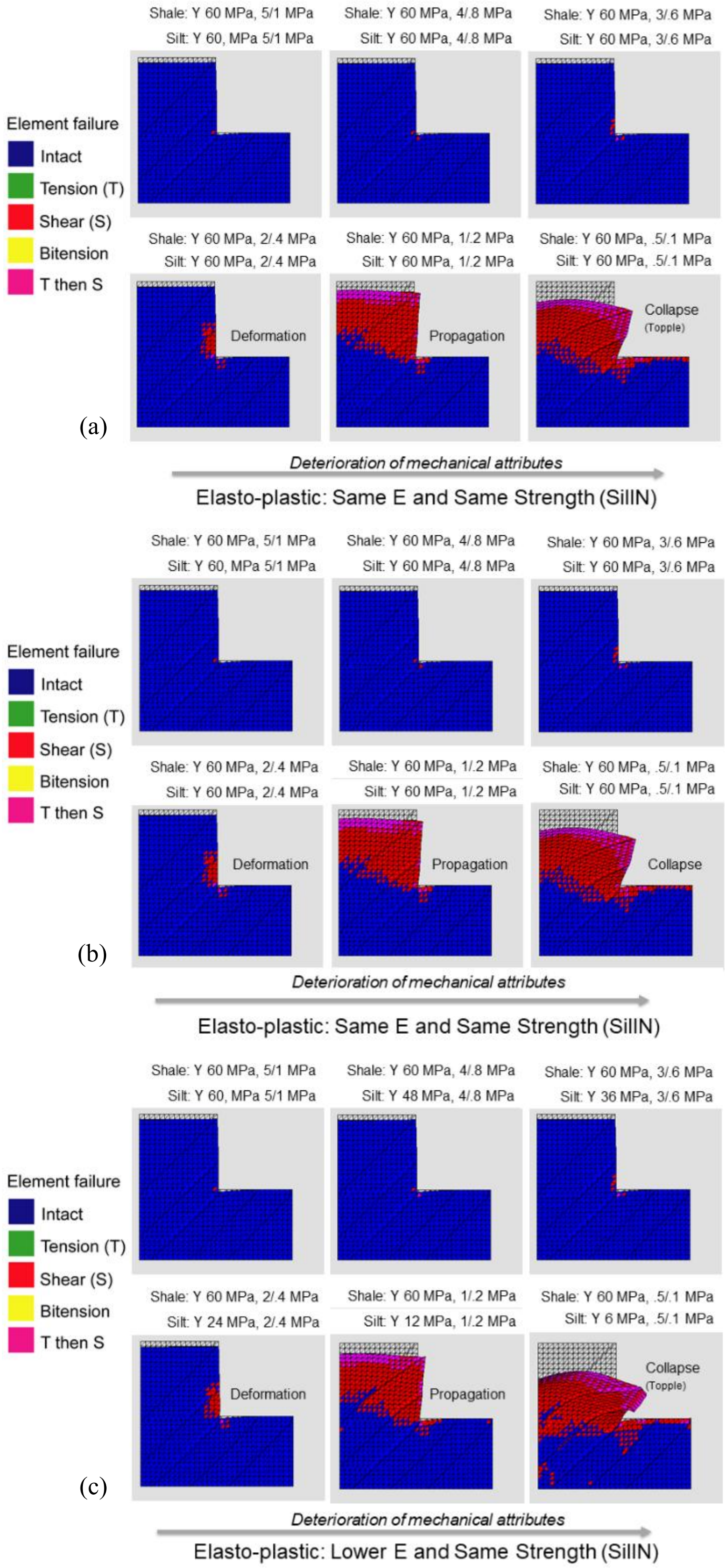

Figure 8: Elasto-plastically analyzed element failure and deformation for in-facing slope (SilIN)

Table 2: Elasto-plastically analyzed deformation and failure in different conditions

			Decrement in engineering properties					
Analysis	**Conditions**	**Rock/ layer**	**0%**	**20%**	**40%**	**60%**	**80%**	**90%**
Elasto-plastic	Same E and Same S	SilHL	-	-	Shear Failure	Notable deformation	Deformation propagation	Collapse
		SiVL	-	-	Shear Failure	Notable deformation	Deformation propagation	Collapse
		SilIN	-	-	Shear Failure	Notable deformation	Deformation propagation	Collapse (Topple)
		SilOUT	Shear Failure at base	Notable deformation	Increased Deformation	Larger deformation	Larger propagation	Larger collapse
	Lower E and Same S	SilHL	No significant difference than Same E and Same S condition					
		SiVL	-	-	Shear Failure	Notable deformation	Deformation propagation	Collapse (Slip)
		SilIN	-	-	Shear Failure	Notable deformation	Deformation propagation	Collapse (Topple)
		SilOUT	Shear Failure at base	Notable deformation	Increased Deformation	Larger deformation	Larger propagation	Solution diverged
	Lower E and Lower S	SilHL	No significant difference than Same E and Same S condition					
		SiVL	-	-	Shear Failure	Notable deformation	Deformation propagation	Collapse (Larger slip)
		SilIN	-	-	Shear Failure	Notable deformation	Deformation propagation	Collapse (Topple)
		SilOUT	Shear Failure at silt later	Larger deformation dominated by T then S	Solution was not conversed. Results are shown for reference	Solution diverged	Solution diverged	Un-converge d results shown for reference

The initiation of shear failure in the SilHL and SilVL (Figs. 6 and 7) aligns with the Mohr-Coulomb failure criterion in soil mechanics. The *E* is crucial for determining the stiffness and load-bearing capacity of these layers. In SilHL, a decrease in the elastic modulus, while strength remains constant, initially shows no deformation; however, reduced stiffness increases susceptibility to plastic deformation and eventual failure. SilVL exhibits similar deformation patterns, indicating that its vertical orientation does not significantly impact its mechanical response.

Complex failure modes, particularly in the SilOUT (Fig. 9), highlight the interaction between shear and tensile stresses, demonstrating "progressive failure," where localized failures can lead to larger-scale instability. When both elastic modulus and strength are diminished, larger slips and complex failure modes indicate that the shale rock mass may experience multiple failure mechanisms simultaneously.

Distinct deformation types—dilatational deformation in SilHL, toppling failure in SilVL and SilIN, and sliding failure in SilOUT—provide insight into stress responses. Toppling failures in SilIN are driven by the overburden pressure and reduced strength of underlying silt, consistent with effective stress principles.

Understanding the relationships among mechanical properties, failure mechanisms, and deformation types enhances slope stability prediction and management, contributing to safer geotechnical engineering practices.

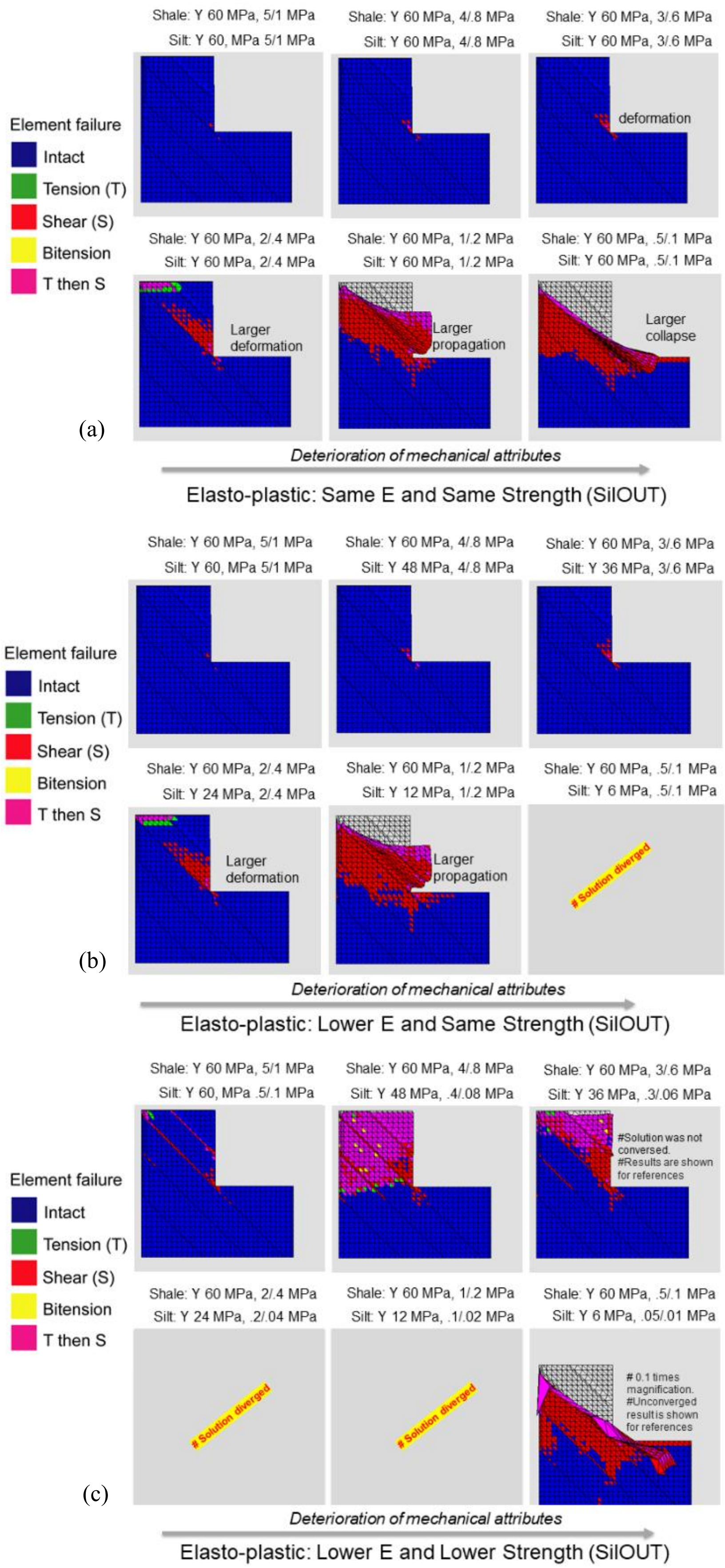

Figure 9: Elasto-plastically analyzed element failure and deformation for out-facing slope (SilOUT)

9. CONCLUSION

The elasto-plastic model employed in this study adequately represents basic failure modes for the shale slopes although it is a continuum type and no special elements are used.

The elasto-plastic analyses revealed a critical failure sequence in the SilHL scenario, where equal elastic modulus (*E*), Unconfined Compressive Strength (UCS), and Tensile Strength (TS) in silt and shale layers lead to a progression from shear to tensile failure, culminating in collapse at a 90% strength reduction. When the silt layer has a lower *E* but equivalent strength to shale, performance remains unaffected. Reducing the *E* and UCS of the silt layer to one-tenth of the shale's strength also shows no significant impact.

In SilVL, similar trends were noted, with slip occurring under comparable conditions. SilOUT displayed initial results akin to SilHL, but tensile failure emerged with distinct modes when the silt layer had a lower *E*.

At the highest degradation levels, different deformation types were identified: dilatational deformation in SilHL, toppling failure in SilVL and SilIN, and sliding failure in SilOUT.

These findings indicate that additional research on particular slope configurations may improve design methodologies and stability assessment in areas susceptible to slope failure within the shale formations of the Chittagong Hill Tracts in Bangladesh.

ACKNOWLEDGEMENTS

Authors would like to express their gratitude to the Department of Petroleum and Mining Engineering, Military Institute of Science and Technology, Dhaka-1216, Bangladesh.

AUTHOR DECLERATION

Authors declare that there is no conflict of interest.

FUNDING INFORMATION

This research was funded by R&D Wing, Military Institute of Science and Technology, Dhaka-1216, Bangladesh.

REFERENCES

Akai, K., & Hori, M. (1978). Fundamental study on instability of tunnel in consideration of post-peak strain softening behavior of rock. Memoirs of the Faculty of Engineering, Kyoto University, 40(2). http://hdl.handle.net/2433/281068

Akoudad, A., Asmi, H. El, Qandil, M. El, Zian, A., Senhaji, A. S., Zandar, S., Darkik, I., Marzouki, A., & Bargach, K. (2024). The Role of Geological and Geotechnical Factors in Shale Slope Instability: Case of Landslides on Road Embankments, Tizi Ouadrene Sector-Rif Extern, Morocco. Iraqi Geological Journal, 57(1), 83–97. https://doi.org/10.46717/igj.57.1B.7ms-2024-2-16

Alam, A. K. M. B., Fujii, Y., Islam, N., Rahman, M. A., Hasan, A. Al, & Hasan, M. A. (2021). Stability of shale at a slope. IOP Conference Series: Earth and Environmental Science, 861(6). https://doi.org/10.1088/1755-1315/861/6/062010

Bishop, A. W. (1955). The use of the slip circle in the stability analysis of slopes. Geotechnique, 15(1), 1–24.

Deris, A. M., Solemon, B., Taha, H., & Omar, R. C. (2020). Determination of influencing factors for slope stability using grey relational analysis (GRA) technique. Systematic Reviews in Pharmacy, 11(4), 202–206. https://doi.org/10.31838/srp.2020.4.29

Ding, Y., Liu, X., Liang, L., Xiong, J., Li, W., Wei, X., Duan, X., & Hou, L. (2023). Wellbore stability model in shale formation under the synergistic effect of stress unloading-hydration. Petroleum Exploration and Development, 50(6), 1478–1486. https://doi.org/10.1016/S1876-3804(24)60481-7

Duncan, J. M., Wright, S., & Brandon, T. (2014). Soil Strength and Slope Stability, 2nd Edition. John Wiley & Sons.

Fell, R., Corominas, J., & Bonnard, C. (2005). Guidelines for landslide risk assessment. International Journal of Landslide, 12(2), 101–115.

Harabinova, S., & Panulinova, E. (2022). Numerical analysis of slope stability. IOP Conference Series: Materials Science and Engineering, 1252(1), 012084. https://doi.org/10.1088/1757-899x/1252/1/012084

Hulagabali, A. (2019). Numerical Analysis of Slope Stability- A Parametric Study. International Journal for Research in Applied Science and Engineering Technology, 7(1), 319–324. https://doi.org/10.22214/ijraset.2019.1056

Lee, C., Kim, J., & Park, H. (2015). Field investigation of slope failures in shale rock masses with silt layers. Engineering Geology, 187, 1–12.

Li, H. (2022). Research progress on evaluation methods and factors influencing shale brittleness: A review. In Energy Reports (Vol. 8, pp. 4344–4358). Elsevier Ltd. https://doi.org/10.1016/j.egyr.2022.03.120

Li, H., Lai, B., & Lin, S. (2016). Shale Mechanical Properties Influence Factors Overview and Experimental Investigation on Water Content Effects. Journal of Sustainable Energy Engineering, 3(4), 275–298. https://doi.org/10.7569/jsee.2016.629501

Mehrabian, A., Nguyen, V. X., & Abousleiman, Y. N. (2019). Wellbore Mechanics and Stability in Shale. Shale. https://api.semanticscholar.org/CorpusID:210737337

Wen, S. L., Hai, B. La, & Chang, Z. W. (2012). Analysis of Influence Factors of Slope Stability. Applied Mechanics and Materials, 34, 256–259. https://doi.org/https://doi.org/10.4028/www.scientific.net/amm.256-259.34.

Zhang, F., Cui, L., An, M., Elsworth, D., & He, C. (2022). Frictional stability of Longmaxi shale gouges and its implication for deep seismic potential in the southeastern Sichuan Basin. Deep Underground Science and Engineering, 1(1), 3–14. https://doi.org/10.1002/dug2.12013

Zhang, Y., Li, X., & Wang, J. (2018). Numerical simulation of slope stability considering silt layers in shale. Computers and Geotechnics, 101, 52–62.